PROCEEDINGS OF SCIENCE

Operation of the CMS Pixel Detector

Andrey Starodumov[*†‡]
IPP, ETH Zurich, Switzerland
E-mail: andrey.starodumov@cern.ch

The CMS pixel detector consists of three barrel layers and two endcap disks on each side of the barrel and has in total 66 million pixels. The operational performance and the status of detector components in collision runs at the LHC in 2010-2011 is presented. The strategies to keep the detector well calibrated for physics needs are discussed.

The 20th Anniversary International Workshop on Vertex Detectors - VERTEX 2011
June 19 - 24, 2011
Rust, Lake Neusiedl, Austria

[*]Speaker.
[†]On behalf of the CMS Collaboration
[‡]On leave from ITEP, Moscow, Russia

PoS(Vertex 2011)009

1. The CMS Pixel Detector

The silicon pixel detector is the central part of the inner tracking system of the Compact Muon Solenoid (CMS) experiment [1] operated at the Large Hadron Collider (LHC) [2] at CERN. The CMS pixel detector allows the precise and efficient reconstruction of the trajectories of charged particles in the region closest to the p-p interaction point and assures the precise reconstruction of interaction and displaced vertices in an environment characterized by high particle multiplicities and high irradiation. The LHC machine is designed to provide collisions of two proton (ion) beams of 7 TeV (2.76 TeV per nucleon) each, with a luminosity of $10^{34}\text{cm}^{-2}\text{s}^{-1}$ ($10^{27}\text{cm}^{-2}\text{s}^{-1}$). In 2010 the LHC started p-p collisions at the center of mass energy of 7 TeV. The instantaneous luminosity has raised rapidly and reached $2\times10^{32}\text{cm}^{-2}\text{s}^{-1}$ in October 2010. By the time of this conference (end of June 2011) the LHC was providing already $2\times10^{33}\text{cm}^{-2}\text{s}^{-1}$ with an average pile-up of about seven hard interactions per one bunch crossing. During so rapidly changing conditions the pixel detector performed very well as will be illustrated later.

The pixel detector consists of three 53.3 cm long barrel layers and two endcap disks on each side of the barrel section, as shown in Fig. 1(a). The innermost barrel layer has a radius of 4.4 cm, while for the second and third layers the radii are 7.3 cm and 10.2 cm, respectively. The layers are composed of modular detector units (called modules) placed on carbon fiber supports (called ladders). Each ladder includes eight modules, shown in Fig. 1(b), consisting of thin, segmented n-on-n silicon sensors of 285 μm thickness with readout chips (ROC) connected by indium bump-bonds [3]. Each ROC [4] serves a 52×80 array of 150 μm$\times$100 μm pixels. The ladders are attached to cooling tubes, which are part of the mechanical structure. The barrel region is composed of 672 full modules and 96 half modules, each including 16 and 8 ROCs, respectively. The number of pixels per module is 66 560 (full modules) or 33 280 (half modules). The total number of pixels in the barrel section is about 48 million.

The endcap disks, extending from 6 to 15 cm in radius, are placed at z = 35.5 cm and z = 48.5 cm. Disks are split into half-disks, each including 12 trapezoidal blades arranged in a turbine-like geometry. Each blade is a sandwich of two back-to-back panels around a U-shaped cooling channel. Rectangular 270 μm thick silicon sensors of five sizes are bump-bonded [5] to arrays of ROCs, forming the so-called plaquettes. Three (four) plaquettes are arranged on the front (back) panels with overlap to provide full coverage for charged particles originating from the interaction point. The endcap disks include 672 plaquettes, for a total of 18 million pixels [6].

2. Operation and status of the Pixel Detector

In 2010-2011 the CMS experiment was taking data in two modes: p-p and heavy ion collisions. The major difference between the two modes is the track multiplicity in a single beam crossing and the Level-1 trigger rate. In p-p collisions on average there are about 3000 pixel hits that were read out at a rate close to 100 KHz. In the heavy ion operation mode the Level-1 trigger rate was 150 Hz while the pixel hit multiplicity was 10 times higher (up to 30000 hits in central Pb-Pb collisions). Changes in the firmware of the Front End Driver (FED) allow to cope with a much larger event size in heavy ion collisions that results in an almost identical performance of the CMS pixel detector in both modes.

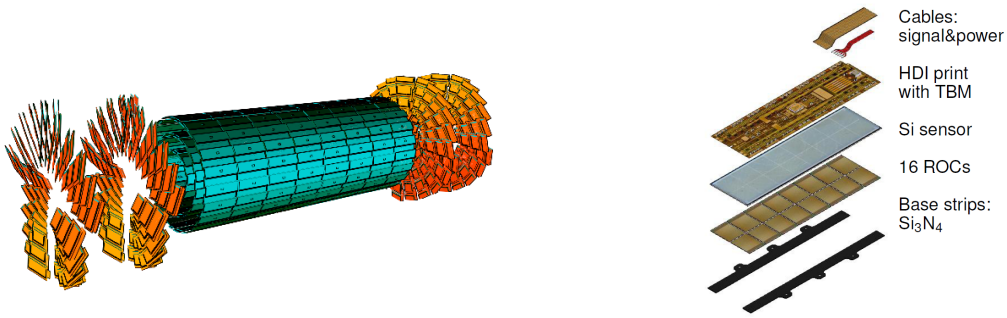

(a) (b)

Figure 1: Sketch of the CMS pixel detector (a) and break-down of the pixel barrel module (b).

The CMS data taking efficiency in both collision modes was above 92%. The pixel detector contributed a very small fraction of about 6% to the total inefficiency of the CMS experiment. The main reason of the dead time coursed by the pixel detector is beam-gas background events characterized by a large amount of pixel hits. In the central collision events with high occupancy occur very rarely while in beam-gas collisions (that are happening a few meters away from the center of the CMS) grazing along the beam axis charged particles create up to 100k pixel hits in one event. When such events coincide with a trigger they must be read out by the corresponding FED channel. The readout time can take up to a few milliseconds that makes event synchronization very challenging. The solution that has been implemented to maintain the synchronization foresees a drop of delayed events. The pixel inefficiency due to the beam-gas background events has reduced substantially but this source still remains a dominant one especially because of permanently increasing luminosity.

During data taking in 2010-2011 the whole pixel detector had 96.9% of functional ROCs: 98.4% in the barrel and 92.8% in the endcap. In the barrel the major reasons to exclude modules from the data taking were broken wire bonds and failed readout electronics. In the endcap, panels were disabled due to slow analog output and lost communication with an optical transmitter (broken laser driver). Some of these problems can be fixed with a modified firmware (efforts are going on) and some other modules could be repaired during a LHC shutdown of a few month.

The level of dead random pixels in functional ROCs is about 10^{-4}. About 6k inefficient pixels were found in calibrations using an internal charge injection. During cosmic ray data taking about 700 pixels were identified as 'noisy' and subsequently masked.

Last year the coolant temperature of the pixel detector was +7.4° C. With increasing radiation damage of the silicon sensors in the future the pixel detector has to be operated at a lower temperature. It is known that several digital to analog converters (DACs) of the chip are temperature dependent. Therefore these DACs have to be optimized for every operational temperature. After the re-optimization of the DAC parameters a set of standard calibrations has to be performed. In January 2011 during the LHC winter shutdown an exercise of the pixel detector calibration has been performed for the coolant temperature of -10° C. It has been demonstrated that the relevant DACs can be re-optimized and all necessary calibrations can be done in a period of a few weeks.

The operation bias voltage is 150 V for barrel modules and is 300 V for endcap panels. The

depletion voltage of an unirradiated silicon sensor is about 50-70 V. A special high voltage (HV) bias scan is performed regularly to monitor changes in the depletion voltage due to irradiation. Since up to now the radiation damage is small enough the change in the depletion voltage is not seen yet. Fig. 2 shows the efficiency measured as a function of the bias voltage for the barrel and endcap. At the operation voltage the efficiency is almost 100%.

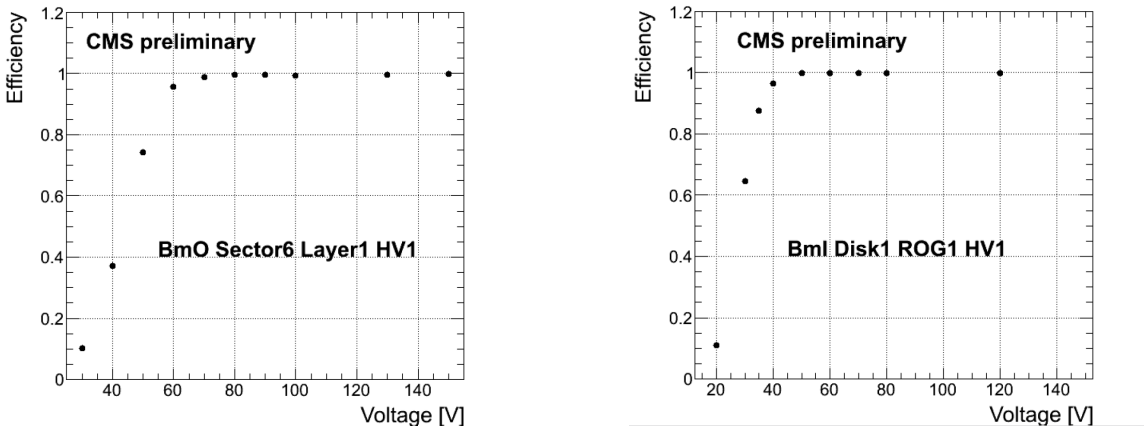

(a) (b)

Figure 2: Pixel efficiency versus bias voltage measured for a few modules in one barrel layer (a) and in a few panels in one endcap readout group (b). The depletion voltage of unirradiated sensors is 70 V in the barrel and 50 V in the endcap.

3. Pixel detector calibrations and performance

To better understand the detector calibrations in the following we briefly describe the pixel data acquisition system (more details in [7]). The readout chain starts in the pixel cell of the ROC, where the signals from individual pixels are amplified and shaped. To reduce the data rate, on-detector zero suppression is performed with adjustable thresholds for each pixel. Only pixels with charge above threshold are accepted by the ROC, marked with a time-stamp derived from the 40 MHz LHC bunch crossing clock, and stored on chip for the time of the trigger latency (about 3.7 μs) until readout. For each Level-1 trigger, an on-detector ASIC, the Token Bit Manager (TBM), initiates a serial readout of the ROCs on one barrel module or endcap panel. Electrical signals from the TBM are translated by the Analog Optical Hybrid (AOH), and transmitted via optical fiber to off-detector electronics. For the full detector, 1214 analog optical links are received in the underground service cavern by forty 36-channel FED VME modules. Each FED has analog optical receivers, flash ADCs, and FPGAs that decode the analog data packets from each channel into pixel addresses and digitized charge information, assemble data packets for each trigger, and buffer the output for transmission of the raw data to the CMS central data acquisition system.

A proper functioning of the pixel detector requires an optimal setting of several parameters. Hence a number of on-line data acquisition calibrations are performed sequentially to adjust each component of the analog readout chain: ROC and TBM output offsets and gains, Analog Optical Hybrid laser bias and gain, FED optoreceiver and channel offsets, and FED flash ADC clock de-

lay. The majority of settings is optimized once and stays unchanged until the detector operating temperature changes or significant radiation damage is accumulated.

The most frequent calibration is an offset adjustment in FED optical receivers that is necessary for keeping a readout signal within the ADC range. Small corrections are made by a FED firmware automatically during data taking. For larger shifts of the offset a special calibration procedure is performed between collision runs.

In the analog readout data packet, six clock cycles are used to encode each hit pixel: the address is amplitude encoded using a six-level scheme over five clock cycles, and the sixth clock cycle gives the pixel charge (Fig. 3(a)). The pixel address calibration is done regularly (although mostly for a check) using an internal (within a ROC) charge injection to a set of pixels in a ROC. A sample set of six address level peaks from one ROC is shown in Fig. 3(b).

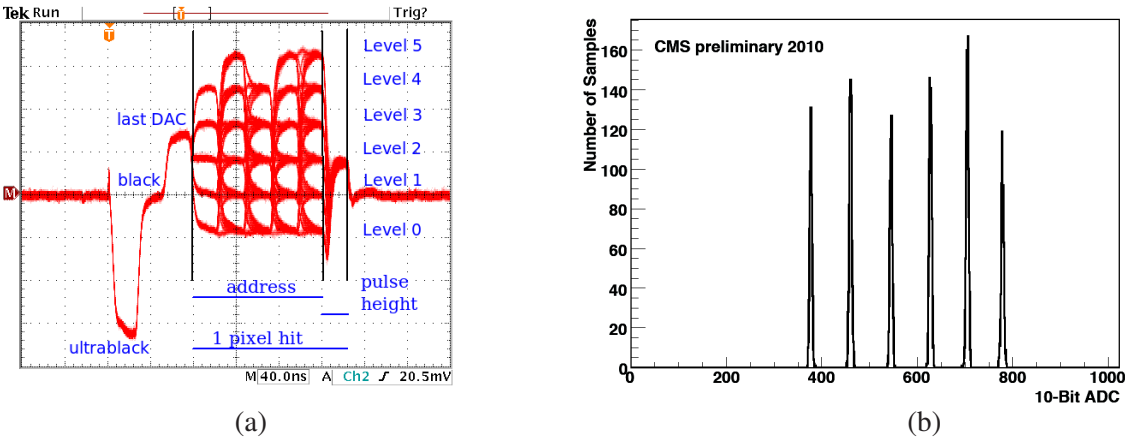

(a) (b)

Figure 3: The oscilloscope view of a single ROC readout (a) and the result of the pixel address calibration of a single ROC (b).

The pixel thresholds are important parameters of the detector. With lower thresholds, lower pixel charges are detectable, hence longer clusters can be reconstructed. The large cluster size ensures the better hit position resolution. The thresholds are controlled at the ROC level by two 8-bit DACs: VcThr is a global chip threshold, and Vtrim is a range within which the threshold is adjusted for individual pixels. The thresholds of individual pixels are adjusted (and equalized within a ROC) using one 4-bit trim value.

The threshold minimization procedure is iterative and a bit different for the barrel and endcap (details in [8]). At each step, VcThr and Vtrim DACs or trim bits are adjusted for a target threshold. The thresholds are measured using charge injection runs by varying the VCal DAC that controls the amount of charge injection. For each pixel, the efficiency as a function of injected charge (S-curve) is fit to an error function. The threshold corresponds to the injected charge (VCal) at which the efficiency is 50%. The noise is measured from the slope of the turn-on region. The limiting factor of this procedure is cross talk: at certain VCal values not only the pixel under tuning but also neighboring pixels are responding. The threshold minimization procedure continues until cross talk is encountered and then thresholds are raised slightly into a stable region. The VCal DAC for every ROC was calibrated using X-ray sources during barrel module tests performed in PSI. An average conversion function is applied for all ROCs in the pixel detector: $Q[e^-] = 65.5 \times \mathrm{VCal}[\mathrm{DAC}] - 414$.

The mean threshold of the pixel detector in the 2010-2011 runs is about 2500 electrons. This is the so-called absolute threshold which the signal pulse crosses regardless of time (bunch crossing). Due to time-walk small signals cross threshold only in subsequent bunch crossings. The in-time threshold is defined as the one that the signal crosses in the same bunch crossing in which the charge was deposited. The in-time threshold is approximately 700-1000 electrons higher than the absolute threshold. Fig. 4 shows the absolute threshold and noise distributions. The noise of each pixel is well below the absolute threshold, so it does not negatively impact the performance of the detector.

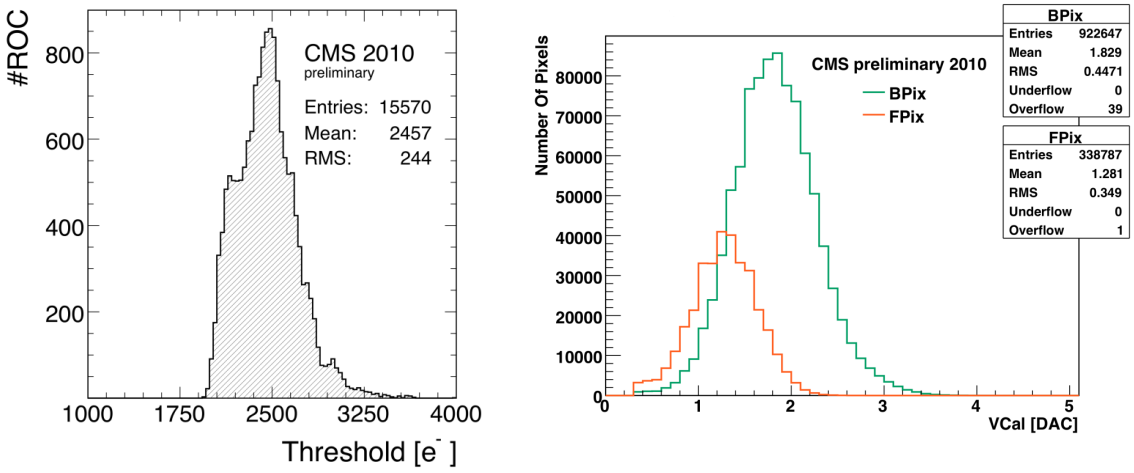

(a) (b)

Figure 4: Absolute threshold (a) and noise (b) distributions in the barrel and endcap. The mean noise is 120 e^- in the barrel (BPix) and 84 e^- in the endcap (FPix).

Conversion of pixel charge measurements from ADC counts to charge units requires calibration of the net response function of the pixel readout chain. This calibration is essential to achieve a precise hit position, as the cluster position is interpolated using the charge information from all pixels in the cluster [9]. The most probable charge deposition for normally incident minimum-ionizing tracks is approximately 21 000 electrons, as expected for fully depleted 270-285 μm thick silicon sensors. This charge is frequently deposited over more than one pixel due to the Lorentz drift and diffusion of collected electrons.

For each pixel the pulse height response in the 8-bit ADC to a given amount of collected charge is measured using the charge injection feature of the ROC (described above). A polynomial of first degree is fit to the ADC versus VCal measurements. The fit is performed in a restricted VCal range to minimize the influence of the non-linearity at high charge. The result of this calibration is a set of two parameters: pedestal and gain, for every pixel. These parameters are very stable and the calibration is performed every few months as a check. The large number of calibration constants requires a compression for use at the High Level Trigger (HLT) and in the reconstruction software. At the HLT both gain and pedestals are averaged per ROC column. In the reconstruction the gain is averaged per ROC column while the pedestals are used for each pixel.

Using the obtained calibration constants the cluster charge distributions from data and MC

simulation are compared. The cluster charge is corrected for the impact angle to the normal track incidence. It is found that the MC simulation describes data quite well: the peak position is correct to the 2-4% level, the width is about 10-15% wider in the simulation.

Pixel hits by design are associated with a particular bunch crossing. Therefore the pixel detector clock should be synchronized with the LHC clock. Due to the different raise time of signals, small charge pulses cross the threshold later than large charge ones. The goal of the time optimization is to set delays such that large pulse height hits are recorded just after the clock transition allowing the maximum time for small pulses to cross the threshold in the same 25 ns bunch crossing window. The parameters to be optimized in the delay scan are the pixel hit efficiency and the cluster size that is sensitive to the small charge hits. The delay scan has been performed in a special calibration run with variable delay steps. The fine scan with 1 ns steps is done close to the right edge of the maximum efficiency/cluster size plateau. Fig. 5 show the result of the delay scan for the barrel and endcap.

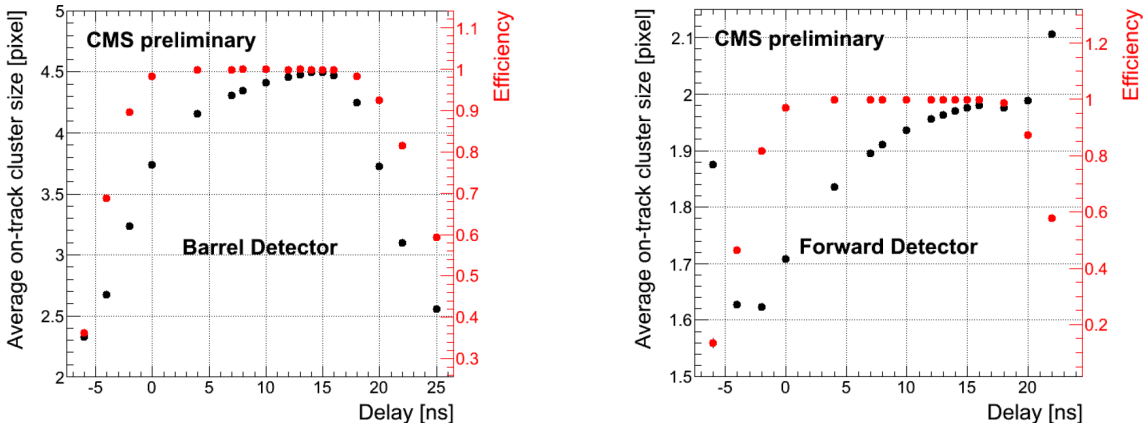

(a) (b)

Figure 5: Cluster size and pixel efficiency measured in the time delay scan in the barrel (a) and endcap (b).

The charge carrier mobility in a silicon sensor depends on the bias voltage, magnetic field strength, temperature and irradiation. Since the resulting deflection by the Lorentz angle θ_{LA} leads to cluster widening in a proper direction, a periodic measurement of the Lorentz angle is necessary. Two methods are used in CMS for the Lorentz angle determination. The minimum cluster size method relays on the fact that the minimum cluster size is created by tracks with an incident angle equal to the Lorentz angle. This method is better suited for tracks with relatively large incident angles such as cosmic ray muons [10]. The grazing angle method [11] is applicable for tracks nearly parallel to the surface that create long clusters. Measurements of the electron average drift distance as a function of the estimated production depth allows to determine the Lorentz angle. Both methods provide consistent results between each other and agree well with the PIXELAV simulation [12]. For example, in the barrel $\tan\theta_{\mathrm{LA}} = 0.405 \pm 0.003$ for data from cosmic ray muons and $\tan\theta_{\mathrm{LA}} = 0.409 \pm 0.002$ ($\tan\theta_{\mathrm{LA}} = 0.391 \pm 0.010$) from p-p collisions obtained with the minimum cluster size method (grazing angle method).

The pixel hit efficiency is an important parameter of the detector to be continuously monitored. All known defective modules are excluded from the analysis. The efficiency is calculated as the

ratio of the number of found hits to the number of expected hits. The expected hit is determined by extrapolating the charged particle trajectory to a pixel module and searching for a hit within 0.5 mm (2 mm) along x (azimuthal direction) and y (longitudinal direction along the beam) of the impact point. Fig. 6 shows the evolution of the hit efficiency versus time and demonstrates that both in the barrel and endcap the efficiency is above 99%. The initial average number of protons per bunch and the number of bunches colliding in the CMS detector are shown in green. An overall decrease of the efficiency in the barrel is about 0.3%. This is an expected dynamic efficiency loss due to the increase in bunch intensity and the number of bunches (that leads to higher occupancy). In the endcap the efficiency stays almost constant within the systematic uncertainty.

The intrinsic hit position resolution is measured using consecutive pairs of hits from the same track in overlapping modules of a single barrel layer. The expected hit position in the x and y directions is determined for both modules using track extrapolation without including hits of the modules under study. Then a double difference of the expected position difference and the measured position difference in two modules is calculated. Such a method reduces the sensitivity to alignment and extrapolation errors. In total 1316 overlapping regions (corresponding to 8.3 million hit pairs) are analyzed. The resulting position hit resolution is $11.2 \pm 0.1\,\mu$m and $26.8 \pm 0.1\,\mu$m in the x and y directions respectively. The agreement between the measured hit position resolution and the one obtained with the CMS pixel detector simulation package PIXELAV [13] is within $1\,\mu$m.

More detailed description of the pixel detector on-line and off-line calibrations can be found in [8] and [14] respectively. The CMS Silicon Tracker performance (including the pixel detector) is reviewed by G. Squazzoni at this Workshop [15].

4. Summary

The CMS pixel detector is performing very well in the rapidly increasing luminosity of p-p collisions and the very high multiplicity environment of heavy ion collisions. The number of functional ROCs is 15342 out of total 15840 that amounts to 96.9% of active channels. The achieved average pixel threshold is about 2500 electrons (limited by cross talk) and the mean noise is less than 150 electrons. The pixel hit efficiency is constantly monitored and up to now stays above 99%. Calibration of the ROC and TBM parameters, optical readout chain, FED parameters, pulse height (ADC-to-Charge) are important for successful detector operation and are performed regularly.. The possible radiation damage is monitored by the high voltage bias scan and soon will be determined through leakage current measurements. The CMS pixel detector, with its pixel hit position resolution of $11-27\mu$m crucially contributes in a high precision primary and secondary vertices reconstruction that is a key factor for many physics analyses carried out by the CMS Collaboration.

References

[1] R. Adolphi *et al.* [CMS Collaboration], "The CMS experiment at the CERN LHC," JINST **0803**, S08004 (2008).

[2] L. Evans (ed.), P. Bryant (ed.), "LHC Machine," JINST **3** (2008) S08001.

[3] C. Broennimann, F. Glaus, J. Gobrecht, S. Heising, M. Horisberger, R. Horisberger, H. C. Kastli, J. Lehmann *et al.*, "Development of an indium bump bond process for silicon pixel detectors at PSI," Nucl. Instrum. Meth. **A565** (2006) 303-308. [physics/0510021].

[4] H. C. Kaestli, "Design and performance of the CMS pixel detector readout chip," Nucl. Instrum. Methods A **565**, 188 (2006).

[5] P. Merkel, "Experience with mass production bump bonding with outside vendors in the CMS FPIX project," Nucl. Instrum. Meth. **A582** (2007) 771-775.

[6] D. Bortoletto [CMS Collaboration], "The CMS pixel system," Nucl. Instrum. Meth. **A579** (2007) 669-674.

[7] D. Kotlinski, E. Bartz, W. Erdmann, K. Gabathuler, R. Horisberger, C. Hormann, H. C. Kastli, B. Meier *et al.*, "The control and readout systems of the CMS pixel barrel detector," Nucl. Instrum. Meth. **A565** (2006) 73-78.

[8] B. Kreis [CMS Collaboration], "The Online Calibration, Operation, and Performance of the CMS Pixel Detector," Nucl. Instrum. Meth. **A650** (2011) 14-18. [arXiv:1101.1989 [physics.ins-det]].

[9] V. Chiochia, "Experience with CMS pixel software commissioning," PoS **VERTEX2008** (2008) 010. [arXiv:0812.0681 [physics.ins-det]].

[10] S. Chatrchyan *et al.* [CMS Collaboration], "Commissioning and Performance of the CMS Pixel Tracker with Cosmic Ray Muons," JINST **5** (2010) T03007. [arXiv:0911.5434 [physics.ins-det]].

[11] B. Henrich, R. Kaufmann, "Lorentz-angle in irradiated silicon," Nucl. Instrum. Meth. **A477** (2002) 304-307.

[12] M. Swartz, V. Chiochia, Y. Allkofer, D. Bortoletto, L. Cremaldi, S. Cucciarelli, A. Dorokhov, C. Hoermann *et al.*, "Observation, modeling, and temperature dependence of doubly peaked electric fields in irradiated silicon pixel sensors," Nucl. Instrum. Meth. **A565** (2006) 212-220. [physics/0510040].

[13] M. Swartz, "CMS pixel simulations," Nucl. Instrum. Meth. **A511** (2003) 88-91.

[14] U. Langenegger [CMS Collaboration], "Offline calibrations and performance of the CMS pixel detector," Nucl. Instrum. Meth. **A650** (2011) 25-29.

[15] G. Squazzoni, these proceedings

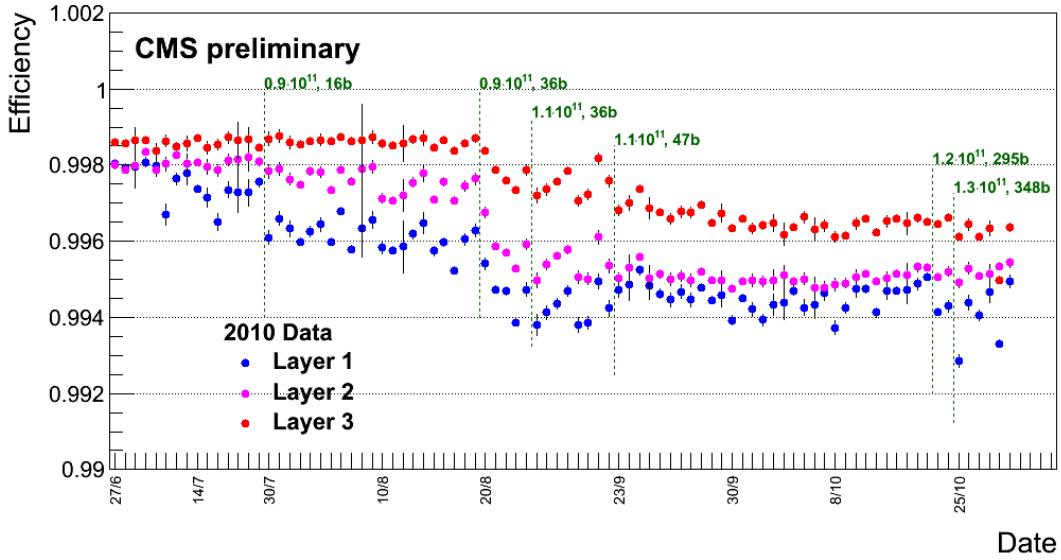

(a)

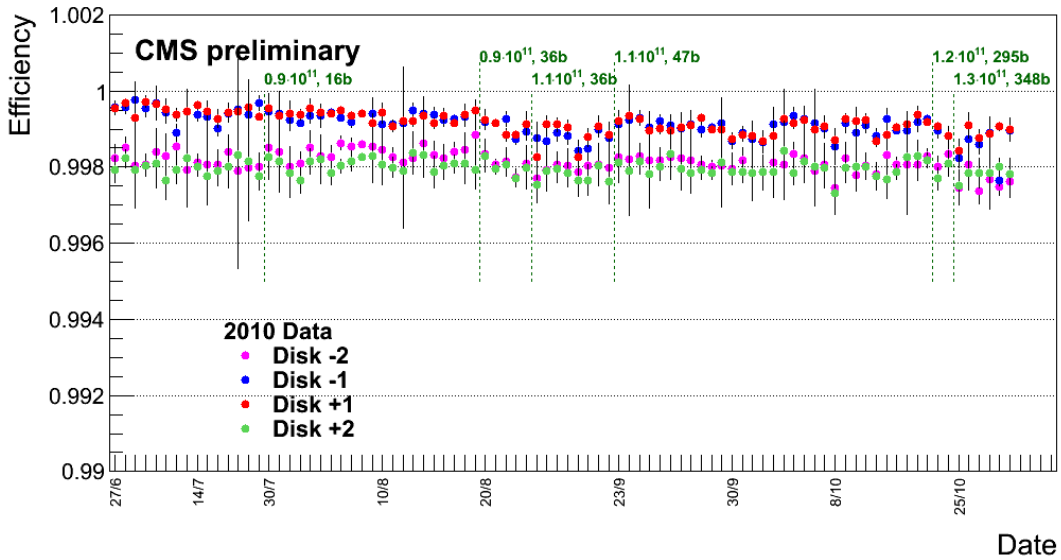

(b)

Figure 6: Pixel efficiency versus time for three layers of the barrel (a) and four disks in the endcap (b). Vertical dashed lines indicate periods of different beam conditions: the initial average number of protons bunch (e.g. $0.9 \cdot 10^{11}$) and the number of bunches (e.g. 16b) colliding in the CMS detector.